Electronic Supplementary Material (ESI) for RSC Advances. This journal is © The Royal Society of Chemistry 2019

Supporting Information

Controllable etching-induced contact enhancement for high-performance carbon nanotube thin-film transistors

*Zhengxia Lv, [adef] Dan Liu, [a] Xiaoqin Yu, [b] Qianjin Lv, [c] Bing Gao, [b] Hehua Jin, *[a] Song Qiu, *[a] Chuanling Men, [c] Qijun Song, [b] Qingwen Li, *[ad]*

a. Key Laboratory of Multifunctional nanomaterials and system integration, Suzhou Institute of Nano-tech and Nano-bionics, Chinese Academy of Science, Suzhou, 215123, P.R. China. E-mail: hhjin2008@sinano.ac.cn; sqiu2010@sinano.ac.cn; qwli2007@sinano.ac.cn

b. School of Chemical and Material Engineering, Jiangnan university, Wuxi 214122, P.R. China.

c. School of Energy and Power Engineering, University of Shanghai for Science and Technology, 516 Jungong Road, Shanghai 200093, P.R. China.

d. School of Physical Science and Technology, ShanghaiTech University, Shanghai 200120, P.R. China

e. University of Chinese Academy of Sciences, Beijing 100049, P.R. China

f. Shanghai Institute of Ceramics, University of Chinese Academy of Sciences, 1295 Dingxi Road, Shanghai 200050, P.R. China

Materials

Raw arc-discharged SWNTs (AP-SWNTs, AP-A204) were purchased from Carbon Solution Inc. Poly[9-(1-octylonoyl)-9*H*-carbazole-2,7-diyl] (PCz, Mw = 45 kDa) was prepared by Suzuki polycondensation with relatively high yield. Other

chemicals and solvents were purchased from Sinopharm Chemical Reagent Co. Ltd. with high purity and received without further purification.

Instruments

UV-Vis-NIR spectra: Optical absorption spectra were measured with a UV-Vis-NIR spectrophotometer (Lambda 750). A sample of the s-SWNTs solution was added into a cuvette (2 mm × 10 mm), and the spectra were measured in the wavelength range of 300–2000 nm.

Morphology characterisation: Atomic force microscopy (AFM) images were recorded on a Veeco Dimension 3100 AFM to characterise the diameter, density and surface morphology of the s-SWNT film, using the tapping mode. Scanning electron microscopy (SEM) images were recorded using an S4800 field-emission SEM instrument from Hitachi (Japan) to characterise the morphology of the s-SWNT film.

Raman spectra: The Raman spectra were measured with a LabRAM HR Raman spectrometer from HORIBA Jobin Yvon equipped with 785 and 633 nm lasers. The Raman spectra of s-SWNT films treated with various etching times were measured under irradiation by the two lasers. The scan range was 10 × 10 μm^2, and the laser spot size was about 0.5 μm.

Electrical measurement: The electrical performances of the devices were tested with a Keithley 4200 semiconductor characterisation system. The bias voltage V_{DS} was -1 V, and the gate voltage V_G was varied from -20 V to 20 V.

Others: The oxygen plasma etching process was conducted with M4L plasma-etching equipment from PVA Tepla (Germany). Ultrasonication was conducted with a

tip-sonicator (SONICS VCX500). The Pd electrodes were prepared by a thermal metal evaporator.

Experimental section

Preparation of high-purity s-SWNT dispersion: First, 100 mg of PCz and 50 mg of AP-SWNTs were mixed in 100 mL of toluene until PCz was totally dissolved. The mixture was sonicated in a water bath for 5 min and ultrasonicated with a tip sonicator for 30 min, with control of the temperature at 20℃ in a circulating water bath. The as-dispersed SWNT solution was first centrifuged at 20,000*g* for 1 h, and the supernatant (80%) was collected to perform further centrifugation at 59,800*g* for 2 h. Finally, the supernatant (80%) was collected as the s-SWNT solution.

Preparation of s-SWNT networks: The commercially purchased SiO_2/Si substrates were ultrasonicated for 5 min with acetone, ethanol and distilled water successively. The wafers were then dried by a stream of nitrogen and heated at 120℃ for 30 min. The clean SiO_2/Si substrates were immersed into s-SWNT dispersion with a concentration of 8 $\mu g \cdot ml^{-1}$ for 2 h to prepare s-SWNT network films at 50℃. The deposited SiO_2/Si substrates were then removed, dried with nitrogen gas, and annealed at 120℃ for 30 min to prepare the s-SWNT networks. The density of the s-SWNT films can be controlled by adjusting the concentration of s-SWNT and the deposition time.

Preparation of s-SWNT TFT: The as-deposited s-SWNT film was annealed at 120℃ for 30 min. The photoresist was then spin-coated under yellow light. The source and drain electrodes of the transistors were patterned by lithography, and plasma etching was applied. The Pd (30 nm) electrodes were deposited via thermal evaporation

followed by lift-off. The channel locations were determined by secondary photolithography. Finally, s-SWNTs outside the channels were removed via oxygen plasma etching to ensure the mutual independence of each device.

1. Evaluation of the s-SWNTs

To evaluate the purity of the sorted s-SWNTs, the absorption spectrum of the s-SWNT dispersion was measured (Figure S1). The M_{11} absorption of metallic SWNTs ranged from 600 to 800 nm. This region displays a deep valley, which means the purity of the sorted s-SWNTs is very high. The parameter Φ is used to quantitatively evaluate the purity of s-SWNTs. The Φ is defined as the ratio of the integrated peak area to the total area of M_{11} and S_{22} regions in the absorption spectra[1,2]. It has been demonstrated that the purity of s-SWNTs is higher than 99% when the value of Φ is higher than 0.4 for the s-SWNTs sorted by polymer. In our previous work, the purity of s-SWNTs sorted by PCz is up to 99.9% corresponding to Φ of 0.42[3]. According to the absorption spectra below, the Φ has calculated to be 0.443, indicating that the purity of s-SWNTs is higher than 99.9%.

To further confirm the purity of the s-SWNTs, the Raman spectrum excited by a 785 nm laser is shown in Figure S2. No signatures of metallic SWNTs can be observed in the radial breathing mode (RBM) band, which ranges from 130 to 180 cm^{-1}, further demonstrating the high purity of the s-SWNTs. As seen in the AFM image in Figure S3, the average length of the as-separated s-SWNTs is about 1.8 μm. Therefore, high-purity s-SWNTs with relatively long length were obtained.

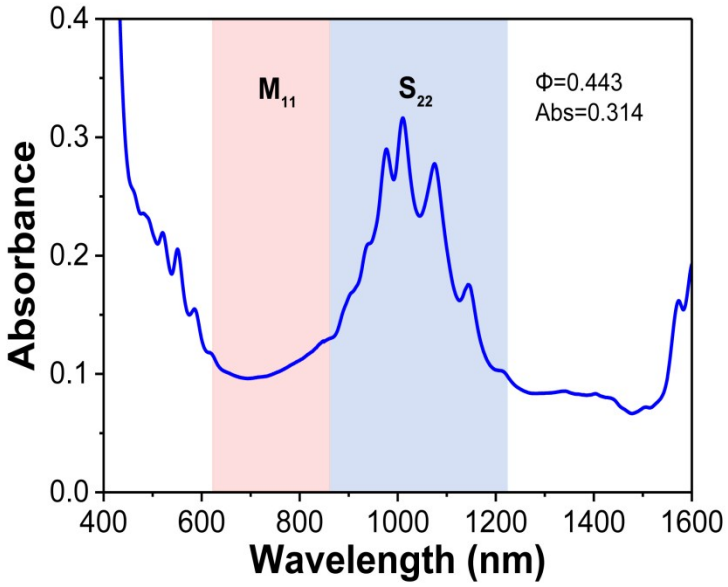

S1. UV-vis-IR absorption of s-SWNTs solution.

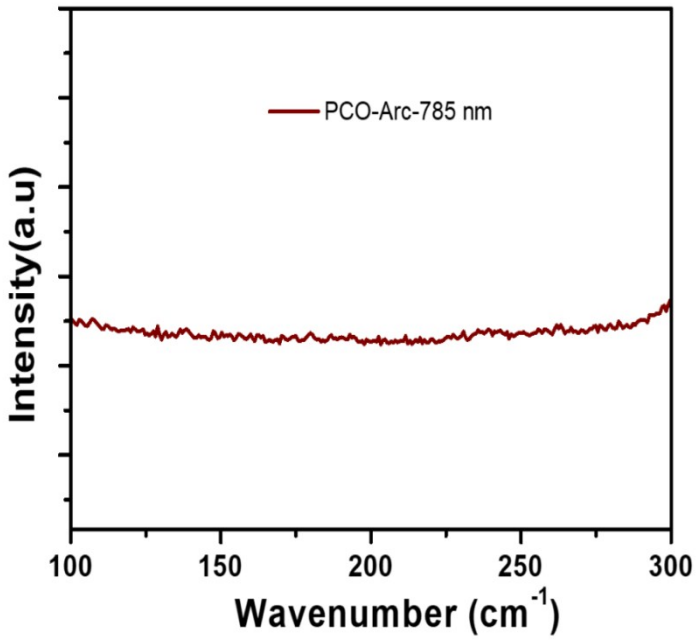

S2. Raman spectrum of sorted s-SWNTs excited by 785 nm laser.

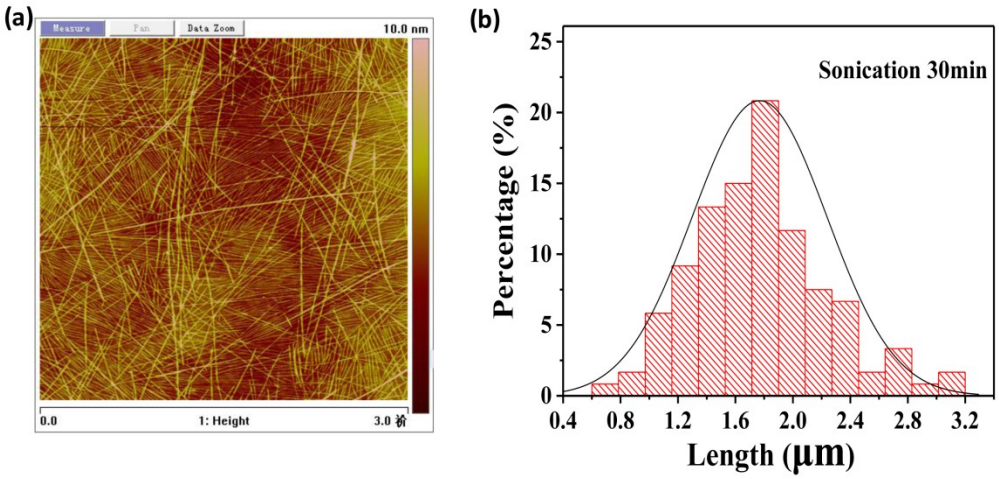

S3. (a) AFM image of sorted s-SWNTs network film. (b) Length histogram of as-separated s-SWNTs. The average length is about 1.8 μm. A total of 120 tubes were counted.

2. Performance and calculation details of as-fabricated TFTs

The variation of on current with etching time can be divided into three stages. In the first stage, from 0 to 20 s, the current increases. In the second stage, from 20 to 90 s, the current begins to decrease. In the last stage, from 90 to 300 s, the current increases again, and the maximum current is reached when the treatment time exceeds 180 s. The on-state current increases from 130 μA (no etching) to 240 μA after plasma etching for 300 s.

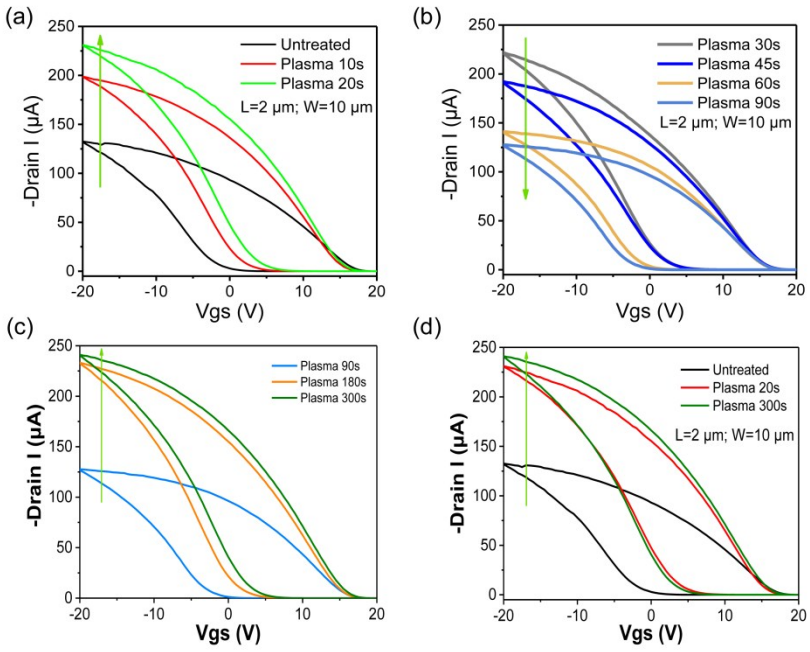

S4. Transfer curves of s-SWNT TFTs with different etching times. (a) 0 s, 10 s, 20 s; (b) 30 s, 45 s, 60 s, 90 s; (c) 90 s, 180 s, 300 s; (d) 0 s, 20 s, 300 s.

Calculation of the mobility of s-SWNT TFTs by the parallel plate model[4]:

The values of charge carrier mobility (μ) were calculated from the I_{ds}–V_{gs} transfer curves in the linear regime (V_{ds} = -1 V) by using the following formula:

$$\mu = \frac{L}{W} \times \frac{\partial I_{ds}}{\partial V_{gs}} \times \frac{1}{C_{ox} \times V_{ds}} \times 10^4$$

Here, L and W are the channel length and width, respectively, defined by the pattern of the electrodes. $\frac{\partial I_{ds}}{\partial V_{gs}}$ was calculated from the transfer curve in the linear regime along the linear axis. C_{ox} is the capacitance of the dielectric layer, $C_{ox} = \varepsilon_0 \times \varepsilon_r \times A/d$, where ε_0 = 8.85 × 10^{-12} F/m; ε_r is the dielectric constant and d is the thickness of SiO_2. Here, the thickness of SiO_2 we used is 100 nm, so C_{ox} is calculated to be 3.45 × 10^{-4} F/m^2.

Time of Plasma (s)	L (μm)	W (μm)	C_{OX} (F/m^2)	$d\,(nm)$	V_{ds} (V)	$\frac{\partial I_{ds}}{\partial V_{gs}}$	Mobility $(cm^2 \cdot V^{-1} \cdot s^{-1})$
0	2	10	3.45E-4	100	-1	-9.72E-6	56
10	2	10	3.45E-4	100	-1	-1.37E-5	79
20	2	10	3.45E-4	100	-1	-1.46E-5	85
30	2	10	3.45E-4	100	-1	-1.40E-5	81
45	2	10	3.45E-4	100	-1	-1.18E-5	68
60	2	10	3.45E-4	100	-1	-1.11E-5	64
90	2	10	3.45E-4	100	-1	-1.01E-5	58
180	2	10	3.45E-4	100	-1	-1.57E-5	91
300	2	10	3.45E-4	100	-1	-1.57E-5	91

Calculation of $2R_c$ by Y function:

The Y function was plotted following the relationship:

$$Y = \frac{I_{ds}}{g_{m}^{1/2}} = (g_{ch} V_{ds})^{1/2} (V_{gs} - V_T)$$

Here, $g_{ch} = \mu(W/L)C_{ox}$ is the $2R_c$-independent transconductance ($2R_c$ being the contact resistance) and is extracted from the slope of the linear region of a plot of Y function versus V_{gs}. The threshold voltage (V_t) is calculated as intercept of the x-axis in

the linear transfer curves. V_{DS} is the voltage between source and drain electrode; I_{DS} is the drain current. $2R_c$ is calculated by the following formula[5,6]:

$$2R_c = \frac{V_{ds}}{I_{ds}} - \frac{V_{ds}}{g_{ch}(V_{gs} - V_T)}$$

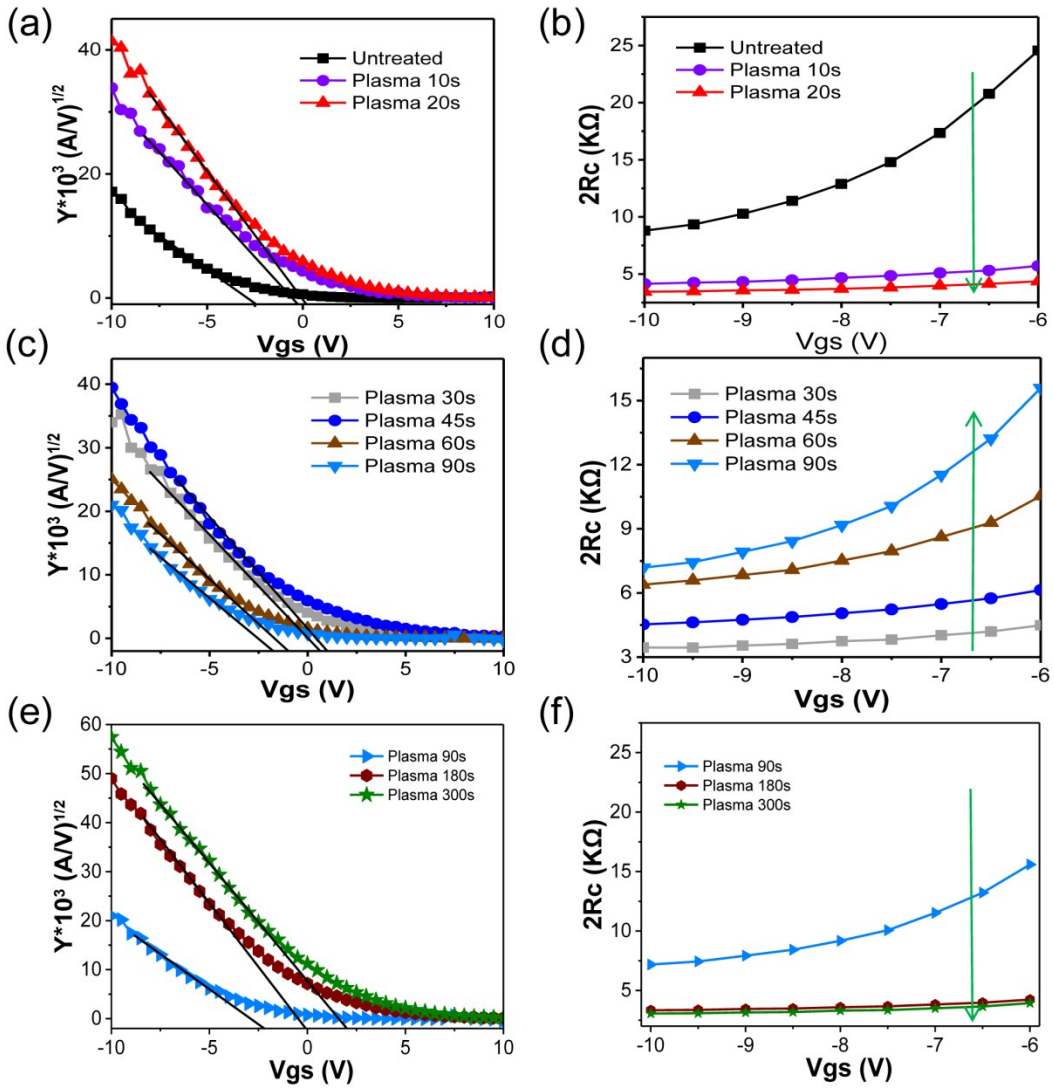

S5. Y-function method fits (a, c, e) and contact resistance ($2R_c$) (b, d, f) for representative TFTs treated by plasma etching for different times.

We calculated $2R_c$ for TFTs treated for various etching times. The change of $2R_c$ of the s-SWNTs TFTs as a function of etching time can be divided into three stages. In the first stage, from 0 to 20 s, $2R_c$ decreases. In the second stage, from 20 to 90 s, $2R_c$ begins to increase. In the last stage, from 90 to 300 s, $2R_c$ decreases again. Under plasma

etching treatment for 300 s, the mean contact resistance decreases from 14.46 kΩ (for the untreated sample) to 3.36 kΩ.

3. Evaluation and reproductivity of as-fabricated TFTs

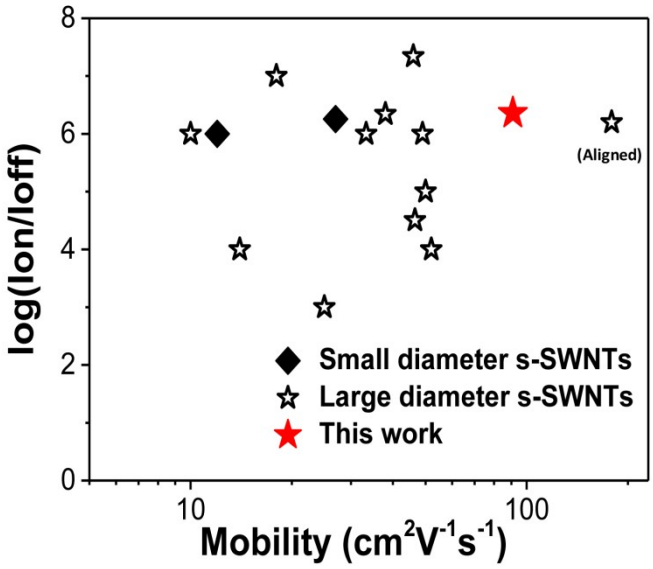

S6. The mobility and on/off ratio of s-SWNT TFTs reported in literatures. Among random s-SWNT-film based TFTs, the performance of the s-SWNT TFT in this work is in the highest level, and comparable with TFTs fabricated on aligned s-SWNT films.

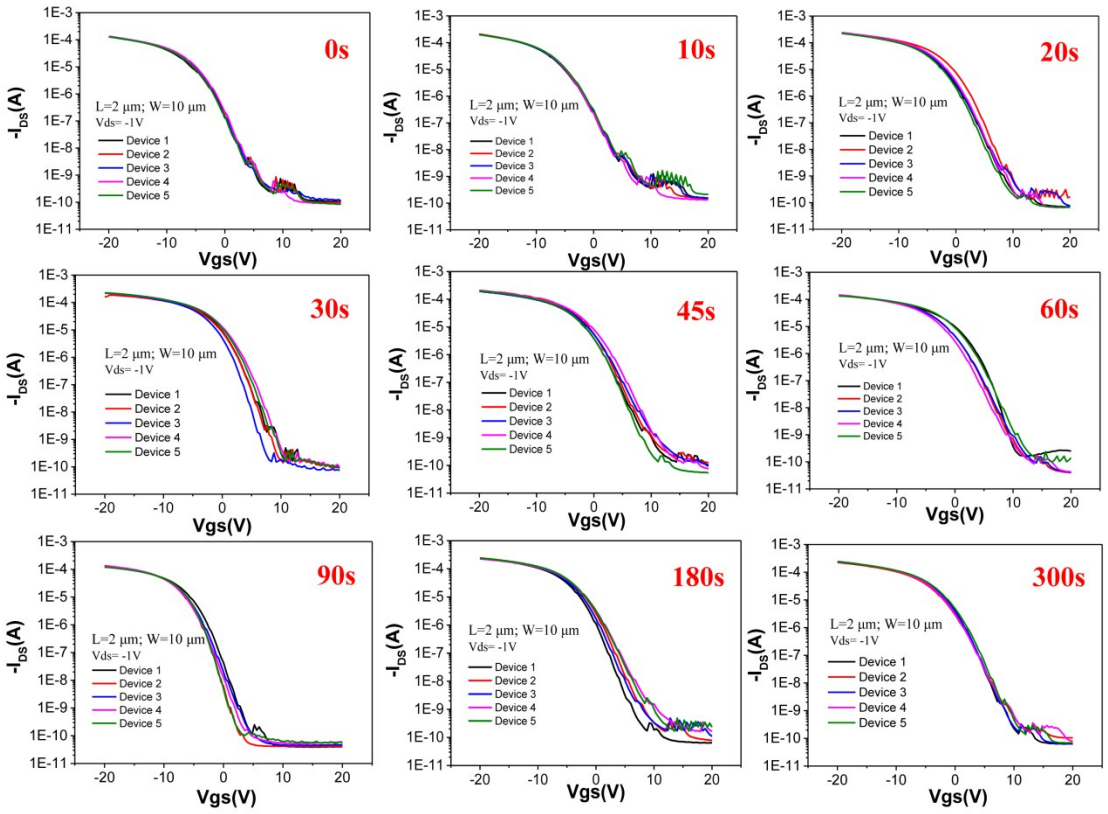

S7. Logarithmic transfer curves of five separated s-SWNT TFTs treated by plasma etching for different times. The five transfer curves under each treatment time are closely overlapped, which denotes that the performance of the s-SWNT TFTs is stable and reliable. Each device was fabricated with a channel length of 2 μm and a channel width of 10 μm; 100 nm SiO_2 was used as the dielectric layer; therefore, the gate efficiency is not high enough. This could be solved by optimising the dielectric layer and the TFTs processing.[7,8]

4. Images of carbon nanotube films with different etching times

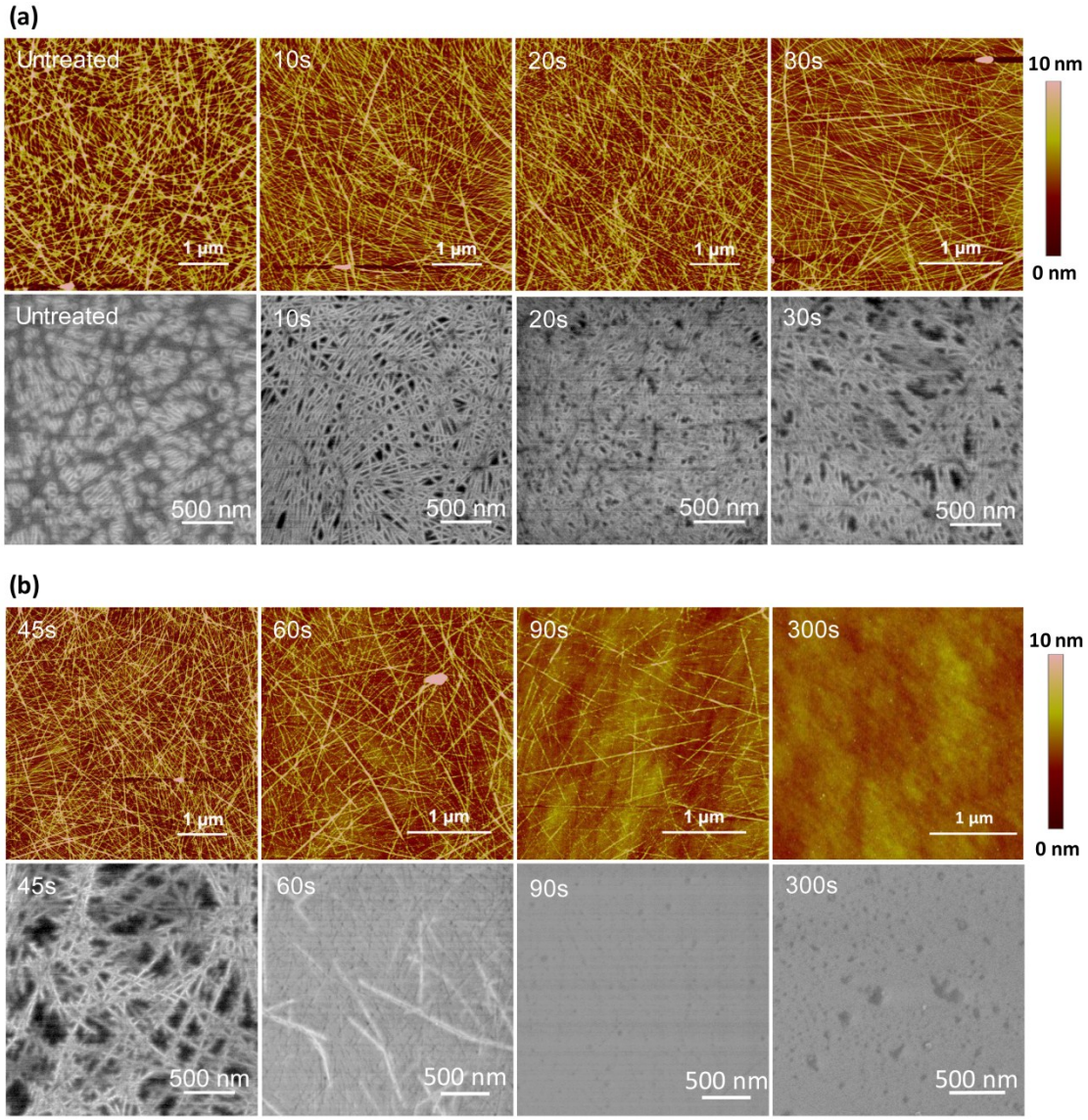

S8. AFM and SEM images of s-SWNT films treated by plasma etching for different times. (a) 0, 10, 20, 30 s (b) 45, 60, 90, 300 s.

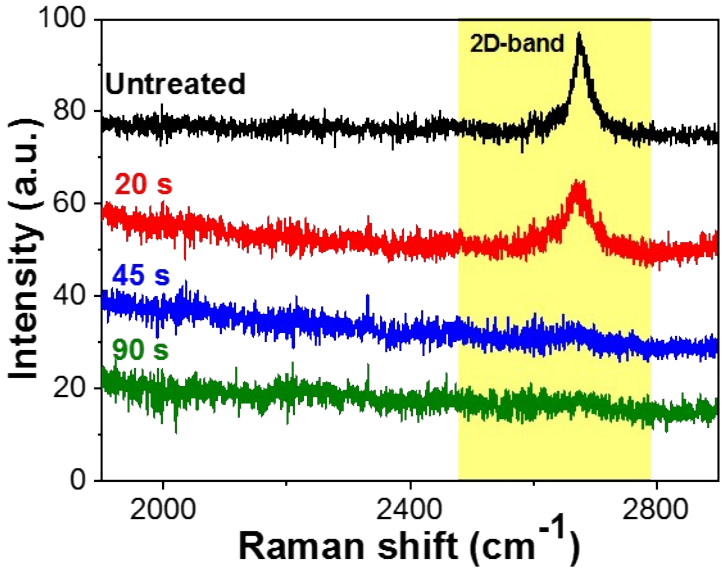

S9. The 2D peaks of s-SWNT films treated by plasma etching for different times, which located at 2650 cm^{-1}.

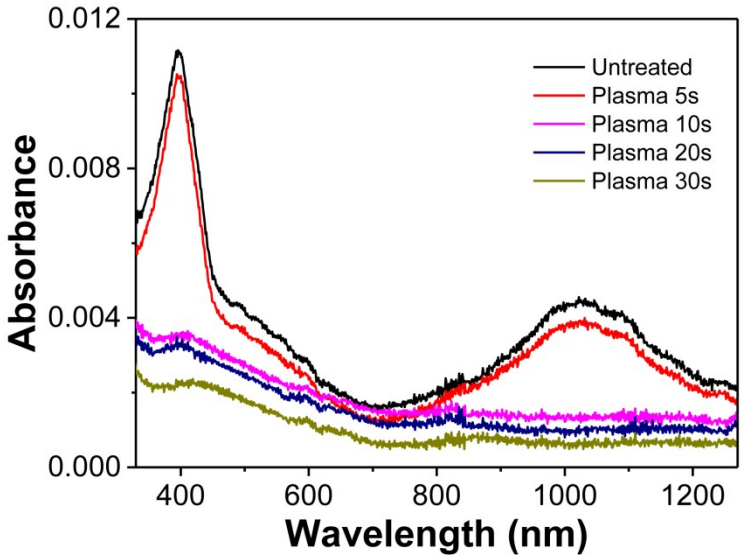

S10. UV–vis–NIR absorption spectra of s-SWNT films treated by plasma etching for different times. To obtain the absorption spectra, the s-SWNT films were deposited on transparent quartz substrates and then etched for different times. The absorption peaks of s-SWNT and PCz gradually disappeared with the increasing of etching time, which

further demonstrated that the plasma etching not only degraded the conjugated polymer but also destroyed the structure of the s-SWNTs.

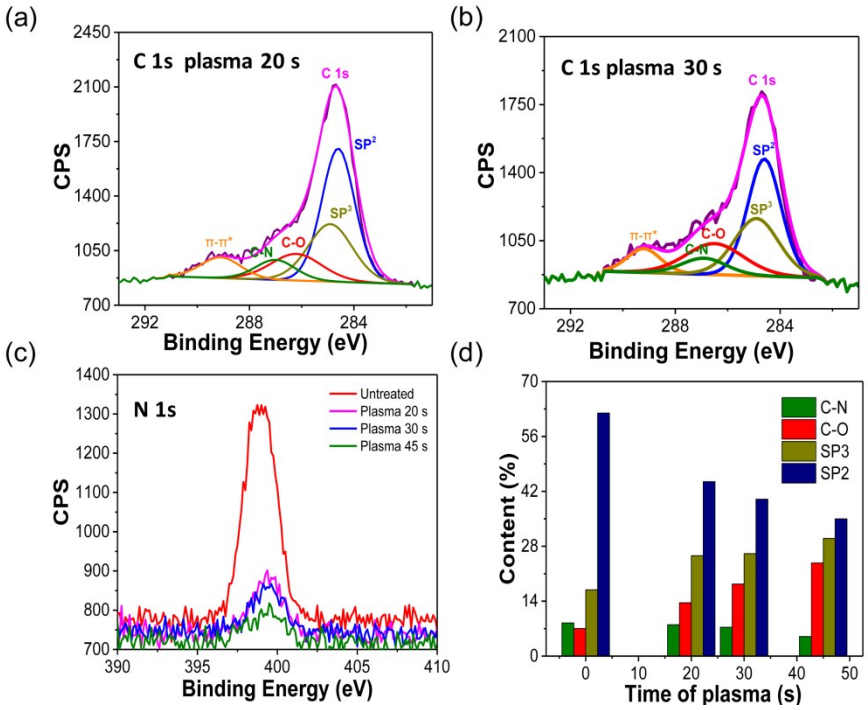

S11. (a)–(b) The deconvoluted C 1s XPS spectra of s-SWNTs treated by plasma etching for 20 s and 30 s. (c) N 1s XPS spectra of the surface of samples treated by plasma etching for 0 s, 20 s, 30 s and 45 s. (d) Contents of chemical bonds on the surface of samples treated by plasma etching for 0 s, 20 s, 30 s and 45 s.

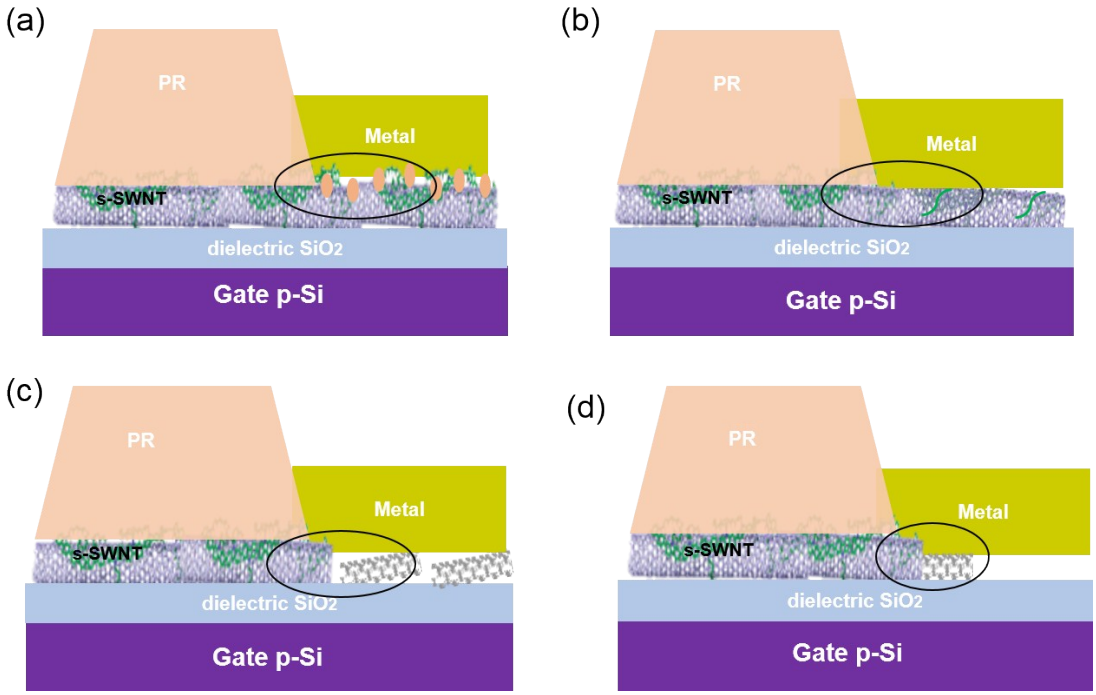

S12. Variation of the contact interfaces between carbon tube and electrode as a function of etching time. (a) t=0s, untreated; (b) $t \leq 20$ s; (c) $20 \text{ s} < t \leq 90$ s; (d) $t \geq 180$ s.

Reference

[1] J. Ding, Z. Li, J. Lefebvre, F. Cheng, J. L. Dunford, P. R. L. Malenfant, J. Humes and J. Kroeger, *Nanoscale*, 2015, **7**, 15741−15747.

[2] I. Pochorovski, H. Wang, J. I. Feldblyum, X. Zhang, A. L. Antaris and Z. Bao, *J. Am. Chem. Soc.* 2015, **137**, 4328-4331

[3] J. Gu, J. Han, D. Liu, X. Yu, L. Kang, S. Qiu, H. Jin, H. Li, Q. Li and J. Zhang, *small*, 2016, **12**, 4993−4999.

[4] S. Z. Bisri, J. Gao, V. Derenskyi, W. Gomulya, I. Iezhokin, P. Gordiichuk, A. Herrmann and M. A. Loi, *Adv. Mater.*, 2012, **24**, 6147-6152.

[5] Q. Cao, S.-J. Han, G. S. Tulevski, A. D. Franklin and W. Haensch, *ACS Nano*, 2012, **6**, 6471-6477.

[6] G. J. Brady, Y. Joo, M.-Y. Wu, M. J. Shea, P. Gopalan and M. S. Arnold, *ACS Nano*, 2014, **8**, 11614-11621.

[7] C. Zhao, D. Zhong, C. Qiu, J. Han, Z. Zhang and L.–M. Peng, *Appl. Phys. Lett.*, 2018, **112**, 053102.

[8] D. Zhong, Z. Zhang, L. Ding, J. Han, M. Xiao, J. Si, L. Xu, C. Qiu and L.–M. Peng, *Nat. Electron.*, 2017, **1**, 40-45.